ELSEVIER

International Immunopharmacology 7 (2007) 392–400

International Immunopharmacology

www.elsevier.com/locate/intimp

Preliminary Report

Inhibition of infection caused by severe acute respiratory syndrome-associated coronavirus by equine neutralizing antibody in aged mice ☆

Lili Zhou [a,1], Bing Ni [b,1], Deyan Luo [a], Guangyu Zhao [a], Zhengcai Jia [b], Liangyan Zhang [a], Zhihua Lin [c], Li Wang [b], Songle Zhang [a], Li Xing [a], Jintao Li [b], Yunfei Liang [b], Xinfu Shi [a], TingTing Zhao [b], Liyun Zhou [b], Yuzhang Wu [b,*], Xiliang Wang [a,*]

[a] *Department of Immunology, Institute of Microbiology Epidemiology, Academy of Military Medical Sciences, Beijing, 100071, China*
[b] *Institute of Immunology, Third Military Medical University, Chongqing 400038, China*
[c] *College of Bioengineering, Chongqing Institute of Technology, Chongqing 400050, China*

Received 19 August 2006; received in revised form 19 October 2006; accepted 20 October 2006

Abstract

The high susceptibility of elderly to severe acute respiratory syndrome-associated coronavirus (SARS-CoV) indicates how crucial it is to protect the elderly by various strategies. Aged BALB/c mice displayed a high susceptibility to SARS-CoV and have been a valuable platform for evaluation of strategies against SARS-CoV infection. In this study, we confirmed the validity of this model using various methods, and verified that equine anti-SARS-CoV $F(ab')_2$ can prevent aged animals from SARS-CoV infection. In a therapeutic setting, treatment with anti-SARS-CoV $F(ab')_2$ decreased viral load more than several thousand folds in the lungs. Thus, this antibody should be a potential candidate for treatment of elderly patients suffering from SARS.
© 2006 Elsevier B.V. All rights reserved.

Keywords: SARS-CoV; Infection; Equine; $F(ab')_2$; Aged; Mice

1. Introduction

The incidence of severe acute respiratory syndrome (SARS) has been controlled, and widespread infections have not re-emerged since the initial outbreak in 2002 and 2003 [1,2]. However, its mysterious animal origins [3] and strong infectivity necessitates further studies on how to control its replication in affected individuals. Retrospective studies have shown that elderly patients with SARS experienced high mortality and morbidity [4–9], suggesting that susceptibility to SARS-associated coronavirus (SARS-CoV) could be correlated with

☆ This work was supported by the National Key Basic Research Program of China ("973" Projects): Funds for the Basic Research of SARS Prevention (2003CB514108), the Key Research Project of the Natural Science Foundation of China (No.30490240), the Outstanding Youth Scientist Foundation of China (No. 30325020), and the National Natural Science Foundation (No. 30571835).

* Corresponding authors. Wang is to be contacted at State Key Laboratory of Pathogen and Biosecurity, Institute of Microbiology and Epidemiology, Academy of Military Medical Science, Beijing 100071, China. Wu, Institute of Immunology, Third Military Medical University, Chongqing 400038, China.

E-mail address: nibingxi@yahoo.com (X. Wang).

[1] Contributed equally to the work.

1567-5769/$ - see front matter © 2006 Elsevier B.V. All rights reserved.
doi:10.1016/j.intimp.2006.10.009

aging. Based upon this observation, Roberts and colleagues established an aged mouse model that has a longer course of virus replication and more severe pathological changes in the respiratory tract than what is observed in young mice [10], which indicates that it is an appropriate animal model paralleling aged humans, in terms of susceptibility to SARS-CoV.

Adoptive antibody transfer has been used to prevent and treat infectious diseases with a long history [11]. It thus provides a candidate strategy for protection of host from SARS-CoV infection. Yo and colleagues found that infusion of convalescent plasma resulted in beneficial clinical outcomes in SARS patients [12]. Subbarao et al verified that passive transfer of SARS-CoV specific antisera reduces pulmonary viral titres in mice infected with SARS-CoV [13], indicating that hyperimmune sera against SARS-CoV could protect against this viral infection. On the other hand, equine antiserum has been successfully used to control various virus infections, such as rabies [14], HBV [15,16], and HIV [17,18]. Based on these evidence of the feasibility that equine antibody can be used for human diseases, we have developed an equine anti-SARS-CoV $F(ab')_2$ that can provide excellent protection from this virus infection, that we previously have tested in a BALB/c model [19].

However, vigorous tests in animal models must be conducted before further clinical trials to insure its efficacy. In this study, we confirmed the aged mouse model using additional assessing methods than previously reported [10], and then tested the equine anti-SARS-CoV antibody in this model, in both preventive and therapeutic settings. As expected, the antibody exhibited a complete preventive effect and a considerable therapeutic role against SARS-CoV infection in this animal model, providing strong evidence for potential application for this antibody in future clinical test.

2. Materials and methods

2.1. Virus and animals

SARS-CoV (strains BJ-01 Genbank accession number AY278488, isolated during 10 Feb to 15 Mar 2003) was maintained in the Institute of Microbiology Epidemiology, AMMS, China, and propagated in Vero cells. The virus was released from infected cells by three freeze-thaw cycles and the titre was determined to be 1.13×10^7 of 50% tissue culture infective doses ($TCID_{50}$)/mL. All operations with SARS-CoV were performed in the Bio-Safety Level 3 (BSL-3) laboratory.

To evaluate the susceptibility of aged BALB/c mice (12–14 months) to SARS-CoV infection, following light anesthetization with isoflurane, 1×10^4 $TCID_{50}$ of 100 μL SARS-CoV particle suspension was administered intra nasally (i.n.) to the animals on day 0. Four mice from each group were sacrificed on days 1, 3, 5, 7, and 9 post infection (p.i.). The lungs of experimental animals were removed and homogenized in a 10% (w/v) suspension of Leibovitz L-15 medium (Invitrogen). The viral titres and copies in the homogenates were then determined using cytopathic effect (CPE) and TaqMan real-time quantitative RT-PCR (qRT-PCR) assays, as described below. The pathology and the localization of SARS-CoV in the lungs of infected animals were determined by pathological observation and immunohistochemistry (IHC), as described below.

To investigate the preventive role of the equine anti-SARS-CoV $F(ab')_2$ against the SARS-CoV infection, following anesthetization, the aged mice were injected intra peritoneally (i.p.) with the anti-SARS-CoV $F(ab')_2$ (1, 2, or 4 mg/kg body weight) or non-immunized normal horse antibody (4 mg/kg body weight), as a negative control, on day −1, the day before viral infection. Twenty-four hours later (day 0), the aged mice were challenged i.n. with 1×10^4 $TCID_{50}$ of SARS-CoV, and were sacrificed on day 2 p.i. The viral titre, copy and localization, as well as the pathologic changes in the infected animal lung were then determined with CPE, qRT-PCR, IHC, and pathological observation methods.

To evaluate the therapeutic role of anti-SARS-CoV $F(ab')_2$ against SARS-CoV infection in the aged mice, the animals received i.p. 100 μL of 1×10^4 $TCID_{50}$ SARS-CoV on day 0, followed by i.p. injection of the $F(ab')_2$ (10, 20, or 40 mg/kg body weight) or normal horse antibody (40 mg/kg) lacking neutralizing activity as a negative control on day 1 p.i. The viral titre, copy and localization, as well as the pathologic changes in the infected animal lung were determined on day 3 and 4 p.i. respectively.

2.2. Cytopathic effect and qRT-PCR assay

The real-time quantitative TaqMan PCR and CPE assays were used to determine SARS-CoV titre and copies in the lungs of SARS-CoV infected or mock infected aged mice. As described previously [19], the number of SARS-CoV N gene copies was determined by qPCR and the CPE assays were conducted on cultured Vero E6 cells.

2.3. Histopathology and immunohistochemistry

Aged mice were anesthetized with isoflurane and euthanized by cervical dislocation on the indicated day following virus administration or anti-SARS-CoV $F(ab')_2$ injections. The lung tissue was fixed with 10% neutral buffered formalin, embedded in a paraffin block, and processed for routine histology and IHC (avidin-biotin peroxidase complex technique, ABC) detections as described by Subbarao et al [13]. For IHC, the purified equine anti-SARS-CoV IgG (1:10,000) was used as the detecting antibody and 3,3'-diaminobenzidine (DAB) as the chromogenic substrate.

2.4. Statistical analysis

Statistical analyses were performed by 1-way ANOVA or/ and multiple comparison (Scheffe) and Student's t test. All graphs represent the mean ± SEM.

3. Results

3.1. Establishment of the animal model susceptible to SARS-CoV infection

Virus titres increased from day 1 p.i., and peaked (about 1×10^8 $TCID_{50}$/g lung tissue) on day 3 p.i.(Fig. 1A). Titres sustained at high level until day 5 p.i. (about 1×10^6 $TCID_{50}$/g), but decreased rapidly thereafter to undetectable levels by day 7 p.i. (Fig. 1A), similar to that observed by Roberts [10]. The qRT-PCR assays verified the course of the viral titre changes (Fig. 1B). On days 1 and 3 p.i., the virus experienced its peak copies of 1×10^{10}/g lung tissue. However, on day 7 p.i., when viral titres were undetectable by CPE assay, several thousand copies of virus could still be detected with qRT-PCR (Fig. 1B).

The severity of pathology was concordant with the amount of virus in the lung. The course of pathological changes was observed systemically. On day 1 p.i., the pathological changes were mild and the lung tissue construction roughly remained normal, except for some small vessel dilatation and congestion, and edema in alveolar spaces (Fig. 2C, arrows), compared with normal mouse lung (Fig. 2A). Viral invasion of bronchial epithelial cells and, to a less extent, alveolar epithelial cells adjacent to the bronchi were observed (Fig. 2D). On day 3 p.i., there was a large degree of inflammatory cell infiltration, mainly involving mononuclear cells and lymphocytes, around the bronchi (Fig. 2E, arrows). We observed focal hemorrhages around small vessels (Fig. 2E, arrowhead), interstitial pneumonia, and shedding of bronchial epithelial cells into the bronchial lumen (Fig. 2E arrow and F). In addition to bronchial epithelial cells, alveolar epithelial cells were infected extensively (Fig. 2F). On day 5 p.i., there was considerable inflammatory cell infiltration that surrounded the bronchi. Shedding of epithelial cells and diffusion of blood cells into bronchial lumen were observed (Fig. 2G arrow and arrowhead). There was obvious effusion in the bronchial lumen, as well. The interstitial pneumonia had become more severe than that observed on day 3 p.i. (Fig. 2G). A large viral load was also observed in animal lungs on this day (Fig. 2H). On day 7, there appeared to be apparent focal consolidation (Fig. 2I arrowhead) and focal necrosis in the lung, accompanied by considerable inflammatory cell infiltration around the bronchi and small vessels (Fig. 2I arrow). However, by this day, the amount of virus had diminished markedly, such that only small amounts of virus could be observed around the bronchi (Fig. 2J). On day 9, consolidations were more obvious than those observed on day 7 (Fig. 2K arrows), accompanied by focal necrosis, inflammatory cell infiltration, and moderate interstitial pneumonia, with still some evidence of effusion in the bronchial lumen (Fig. 2K). However, almost no virus could be observed on this day (Fig. 2L).

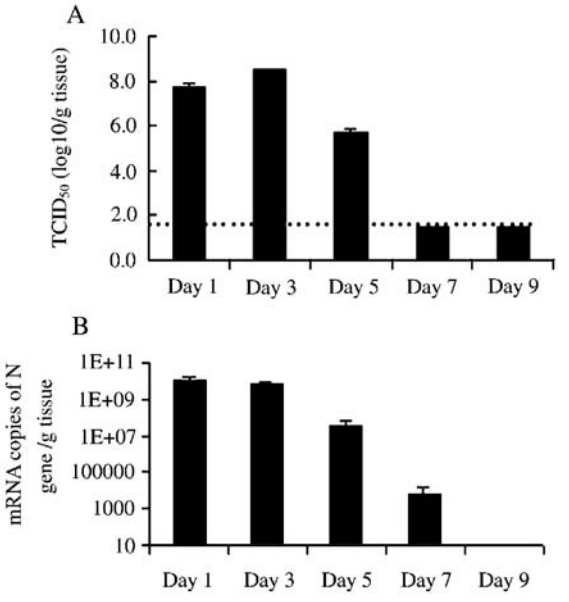

Fig. 1. Replication of SARS-CoV in the lung tissue of aged mice. Aged mice were administered 1×10^4 $TCID_{50}$ of SARS-CoV on day 0. Virus titres and copies in lung homogenates were measured at the indicated days p.i., and shown as mean values, calculated from four mice per day. Error bars indicate standard errors. Panel A: CPE assays of virus titres in aged mice lungs. Virus titres are expressed as $\log_{10}TCID_{50}$ per gram of lung tissue. The lower limit of detection of virus in a 10% w/v suspension of lung homogenate is 1.5 $\log_{10}TCID_{50}$ per gram (dotted line). Panel B: TaqMan real-time RT-PCR assays of virus copies in infected aged mice lungs. Copies of N gene derived from SARS-CoV were expressed as absolute copies of N gene per gram of lung tissue.

3.2. Prevention of SARS-CoV infection by equine anti-SARS-CoV $F(ab')_2$ fragments

Because the results from the above experiments demonstrated that the viral titres in virus-inoculated animal lungs were highest during days 1–5 p.i., we injected the indicated amounts of equine anti-SARS-CoV $F(ab')_2$ into mice on day-1 (minus 1) and challenged them with 1×10^4 $TCID_{50}$ of SARS-CoV on day 0. Then, we investigated the protective roles of antibody against virus infection on day 2 p.i. and whether the protective role was antibody dose-dependant. CPE assays showed that 4 mg/kg body weight of the antibody could completely neutralize the virus in inoculated animal lungs (Fig. 3A). Even at half the effective dosage (2 mg/kg), the antibody provided remarkable protective effect (Fig. 3A). In contrast, injection of non-immunized normal equine $F(ab')_2$ at 4 mg/kg did not protect the aged mice against SARS-CoV infection, similar to the virus positive control (Fig. 3A). Accordingly, the qRT-PCR assay also demonstrated that 4 mg/kg body weight of the antibody could completely clear the inoculated virus from the experimental lungs, as we could not detect the SARS-CoV N gene in the lung homogenates at this dose (Fig. 3B). Similar to our observation

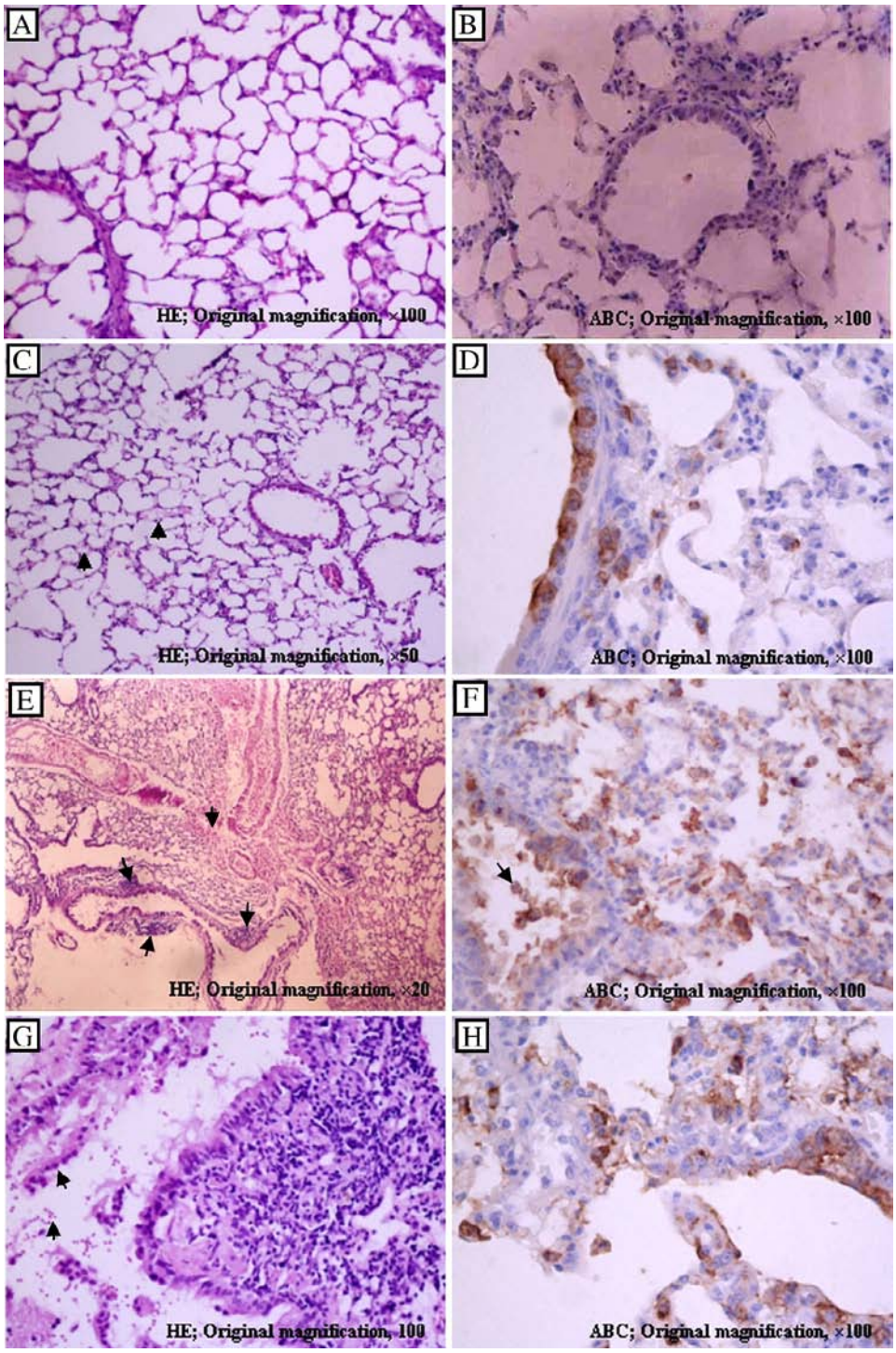

Fig. 2. Histopathological observations and IHC assays on the lung tissue of aged mice with SARS-CoV infection. Aged mice were administered 1×10^4 $TCID_{50}$ of SARS-CoV on day 0. The experimental animal lungs were fixed with formalin and then stained with hematoxylin-eosin (HE) for pathological observation, or examined with IHC assay with anti-SARS-CoV $F(ab')_2$ as the primary antibody (1:10,000) and DAB as a chromogenic substrate. Lung tissue from normal mice (A) and from study animals on days 1 (C), 3 (E), 5 (G), 7 (I), and 9 (K) p.i. was examined by means of HE staining. The distribution of SARS-CoV in the affected animal lungs was determined using IHC in normal animal lung (B) and in animals inoculated with the virus on days 1 (D), 3 (F), 5 (H), 7 (I), and 9 (L) p.i. To assay the therapeutic effect, animals were treated with 40 mg/kg of antibody after viral exposure and the lungs were analyzed on day 4 p.i. (Panel M and N). The selected figures are representative of the four animals per group.

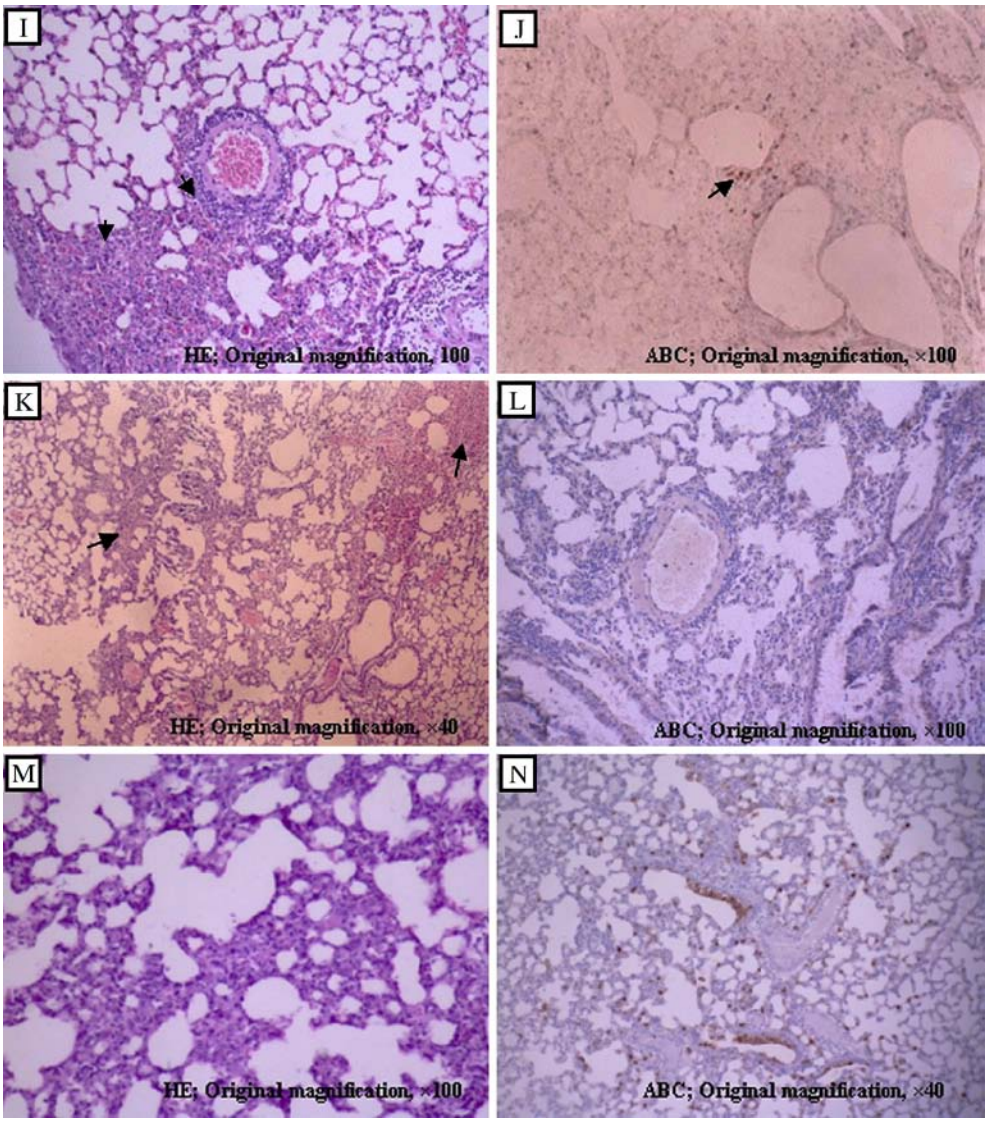

Fig. 2. (*continued*).

above, treatment with 2 g/kg body weight of antibody resulted in about 100-fold decrease of virus load in inoculated animal lungs (Fig. 3B). In the control group, we could still detect about 10^{10} copies of N genes, which did not differ from those observed in the virus positive control group (Fig. 3B).

3.3. Therapeutic role of equine anti-SARS-CoV F(ab')$_2$

The therapeutic role of equine anti-SARS-CoV antibody against SARS-CoV infection, and whether this role is antibody dose-dependant, were investigated further in this same aged mouse model. Each aged mouse was inoculated with 1×10^4 $TCID_{50}$ SARS-CoV on day 0, and received an i.p. injection of the indicated dose of F(ab')$_2$ on day 1. Because the half-life of the prepared F(ab')$_2$ fragments is 60 h (as determined in rats, data submitted), we measured the therapeutic role of the antibody on days 3 and 4 p.i. When the equine neutralizing antibody was administered after virus inoculation, 40 mg/kg of antibody could relieve the pathological lesions and viral load in animal lungs (Panel 2M and 2N) on day p.i. 4, compared to virus control (Panel 2E–H). On the same day, animal lungs showed mild to moderate interstitial pneumonia and lung consolidation, but the morphological structure of the lung was roughly normal (Panel 2M and 2N). The CPE assays indicated that 40 mg/kg of F(ab')$_2$ could exert a significant therapeutic effect on the inhibition of SARS-CoV infection, because animals protected with this dose of SARS-CoV specific antibody experienced a markedly decreased viral load in their lungs, compared with the negative antibody controls ($p<0.01$)(Fig. 4A). As expected, the therapeutic efficiency of

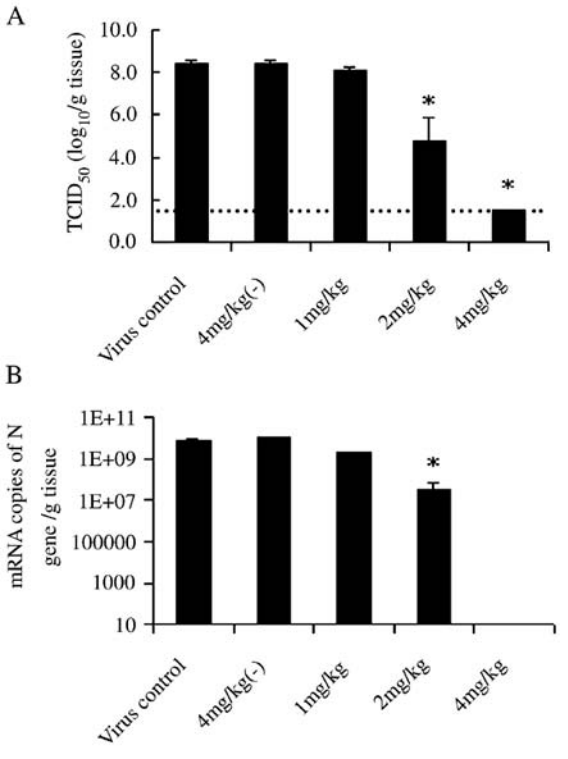

Fig. 3. Prevention of SARS-CoV infection in aged mice. The indicated amount of equine anti-SARS-CoV F(ab')$_2$ fragments was injected i.p. into aged mice on day-1 and the animals were challenged with 1×10^4 $TCID_{50}$ of SARS-CoV i.n. on day 0. Virus titres and copies in lung homogenates were measured on day 2 p.i., and shown as mean values, calculated from four mice per group. Error bars indicate standard errors. Panel A: CPE assays of virus titres in aged mice lungs. Virus titres are expressed as $\log_{10}TCID_{50}$/g lung tissue. The lower limit of detection of virus in a 10% w/v suspension of lung homogenate is 1.5 $\log_{10}TCID_{50}$ per gram (dotted line). Panel B: qRT-PCR assays of virus copies in experimental animal lungs. Copies of N gene derived from SARS-CoV were expressed as absolute copies of N gene/g of lung tissue. The antibody-negative control mice received the indicated amount of non-immune equine antibody. *$p<0.01$ (1-way ANOVA assay) compared with 4 mg/kg of non-immune equine antibody control.

this kind of antibody on day 4 was similar to that on day 3 (Fig. 4A). In contrast, the negative antibody control, non-immune equine F(ab')$_2$, did not provide any neutralizing effect on the virus (Fig. 4A). Our qRT-PCR assays further confirmed those results in CPE assays (Fig. 4B). The dose of 40 mg/kg F(ab')$_2$ fragments could partially, but significantly decrease viral copies in infected animal lungs, about 1000 folds when compared to the untreated animals (Fig. 4B).

4. Discussion

Roberts has established the aged mouse model for infection of SARS-CoV (Urbani isolate) by using pathological observation and CPE assay [10]. As this aged mouse model has not been studies extensively, we employed additional methods to assess and verify the aged mouse model. We were able to infect aged BALB/c mice with SARS-CoV (BJ-01 strain) through i.n. inoculation, and could demonstrate the virus replicated effectively in the lungs of infected animals. Using the CPE assay, we observed rapid virus propagation after day 1 p.i., which peaked on day 3 p.i. (1×10^8–10^9 $TCID_{50}$/g), and thereafter diminished gradually. However, it still sustained high titres (about 10^6 $TCID_{50}$) on day 5 p.i., similar to that reported by Roberts [10]. Quantitative PCR results

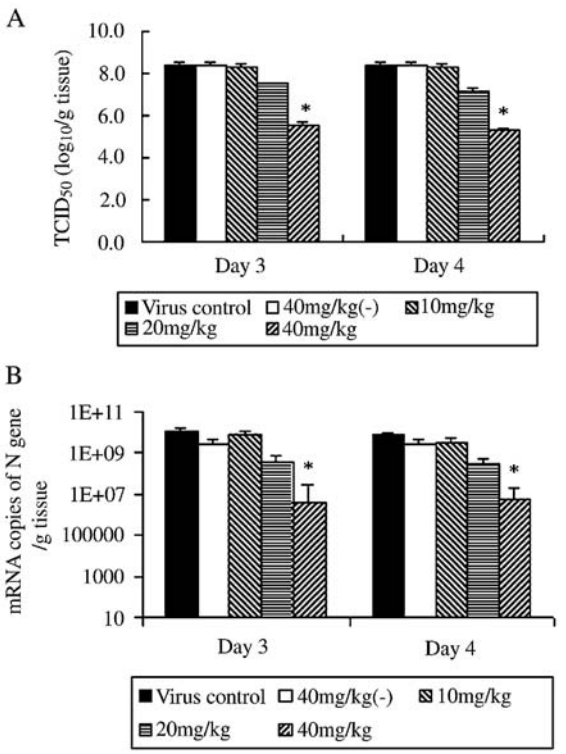

Fig. 4. Therapeutic effect of equine anti-SARS-CoV F(ab')$_2$ on SARS-CoV infection in aged mice. The animals were challenged with 1×10^4 $TCID_{50}$ of SARS-CoV on day 0 i.n. and protected with i.p. injection of the indicated amount of anti-SARS-CoV F(ab')$_2$ fragments on day 1 p.i. Virus titres and copies in lung homogenates were measured on the indicated days, and shown as mean values, calculated from four mice per group. Error bars indicate standard errors. Panel A: CPE assays of virus titres in aged mice lungs. Virus titres are expressed as $\log_{10}TCID_{50}$ per gram of lung tissue. The lower limit of detection of virus in a 10% w/v suspension of lung homogenate is 1.5 $\log_{10}TCID_{50}$ per gram (as shown by dotted line). Panel B: qRT-PCR assays of virus copies in experimental animal lungs. Copies of N gene derived from SARS-CoV were expressed as absolute copies of N gene per gram of lung tissue. The antibody-negative control mice received the indicated amount of non-immune equine antibody. *$p<0.01$ (1-way ANOVA assay) compared with 40 mg/kg of non-immune equine antibody control.

showed that expression pattern of the viral N gene paralleled the viral titre changes, confirming our results from the CPE assay. Though we failed to detect any virus present on day 7 p.i. using the CPE assay, qRT-PCR showed thousand copies of virus in the lungs of some animals (2/4) (Fig. 1B). This could reflect the sensitivity difference between the CPE and real-time RT-PCR assays. CPE assay is not an absolute quantitative method, thus it cannot provide concrete virus number in certain sample. On the other hand, Taqman fluorescent qPCR assay can detect even single copy gene [20], thus it can provide more details for the molecular mechanism of SARS-related pathogenesis and the evaluation of various intervening strategies than CPE method can. Therefore, in this study we demonstrated the usefulness of qRT-PCR over the CPE assay to accurately determine virus replication, which allowed us to establish a model for SARS-CoV infection.

Surprisingly, Roberts observed the illness in SARS-CoV infected mice [10], but in this study, we could not observe the symptom development related with SARS-CoV infection in aged mice. We speculate that this may be related to the observation and calculation methods for clinical disease and surrounding factors such as feeding, since we observed that the body weight of some normal control mice could increase or decrease 1–2 g during the one-week observation.

Concordant with the observation of Roberts' [10], we found definitive pathological changes in the lungs of infected animals. Furthermore, we have also systematically defined the pathological changes in infected animal lungs. The typical pathological changes were interstitial pneumonia (when large amounts of virus infected the bronchi epithelial and alveolar cells) (Fig. 2C–H), and multiple focal lung consolidations (when virus titres began diminishing) (Fig. 2I–L), when compared to normal mouse controls (Fig. 2A and B). The two major pathological changes were similar to those observed in patients with SARS [21–26].

Although detailed tissue studies of SARS-CoV infection in patients' lung have not been performed, based on the symptoms and signs, indirect evidence including radiographic features, and partial direct evidence including throat wash and autopsies [8,27,28], it appears that the pathological course of infection is similar to that observed in aged mice. Thus, even though we did not detect evidence of disease development in infected mice, detailed tissue studies reported here support the validity of the aged mice model. Importantly, the close correlation between the degree of pathological change and virus titres or virus copies in the aged mouse model [10] indicates that the mouse model serves as credible system to investigate the effectiveness of various interventions against SARS-CoV infection.

A recent study of the humoral immune response of SARS patients indicated that patients with a longer course of illness showed a lower neutralizing antibody response than patients with a shorter illness duration [29]. This indicates that neutralizing antibodies in patients play a pivotal role in SARS-CoV clearance *in vivo*. Accordingly, we have generated equine anti-SARS-CoV $F(ab')_2$ and shown significant protection against SARS-CoV infection in a young BALB/c mouse model [19]. Complete neutralization of the virus in infected aged mouse was achieved with 4 mg/g body weight of this antibody in a preventive setting (Fig. 3). In addition, the protected animals did not show pathological changes in their lungs (data not shown). Similar results were also observed in young mice that received comparable amount of the equine antibody [19]. Even though we did not examine the therapeutic role of this antibody in young mice due to the short infection endurance (about 3 days) [19], we have achieved great success using this antibody to treat SARS-CoV infection in aged mice, which have longer infection endurance (about 5 days) (Fig. 4). This level of protection observed (1000-fold decrease in viral load), although not complete, is remarkable, considering that the circulating antibodies can only neutralize the extracellular SARS-CoV. Our results also suggest that in therapeutic settings it might be necessary to combine passive antibody transfer with other methods such as antiviral drugs and vaccines.

The ideal immunoglobulin for adoptive transfer would be of autologous or homologous origin for the lowest anti-antibody response and humanized MAb can be taken as a good candidate in this respect. However, the issue of low MAb yield needs to be overcome when used in clinics. Polyclonal immunoglobulins can surmount the obstacle in antibody production. Another potential advantage using polyclonal antibody is the broad antigenic coverage and reduced likelihood of emergence of escape mutants. Among the various heterologous antibody approved, equine antibody is one of the appealing choices [11]. In view of the convenience of horse feeding and serum availability at the same time, the equine antibody treatment approach offers the advantage over monoclonal antibody. In spite of the availability of human or humanized MAbs in anti-SARS-CoV research [30–34], equine antibody is still an attractive candidate for the prevention and treatment of SARS patients.

One potential problem with the equine immunoglobulins treatment is immunogenicity, but various measures can be taken to reduce the immunogenicity to a

tolerable level, such as removing the Fc fragment. Our experimental data (submitted) from 18 monkeys that received intravenous injection of the truncated immunoglobulin (removed the Fc fragment) showed mild stimulation in their immune response. All animal subjects survived the injection, and the motivated host secondary lymphoid organs, the spleen and lymph node, recovered after 3 weeks post injection withdraw. Since the host anti-F(ab')$_2$ antibody appears at 2 weeks post the F(ab')$_2$ administration (submitted data) and the almost complete neutralization of extracellular virus, application of this antibody will inhibit other normal tissue from infection, as shown in this study, thus preventing further transmission. This will allow the host's immune system to clear the remaining virus or provide the chance for the intervention of other strategies such as antiviral drugs, RNAi and vaccines to ultimately eliminate the virus form the host.

In summary, we have established and verified the aged mouse model, and confirmed that it parallels the pathological change pattern that occurs in older human patients suffering from SARS. More importantly, the equine polyclonal antibody used in this study exhibited an excellent therapeutic effect post virus exposure. Together with its proven protective role against SARS-CoV infection in young mice [19], we have provided strong evidence for the therapeutic application for this antibody in both treatment and prevention of SARS.

Acknowledgement

We appreciate Dr. Henry Teng (Cellular and Molecular Division, Toronto Western Research Institute, Canada) for the correction of this manuscript.

References

[1] Enserink M, Normile D. Infectious diseases. Search for SARS origins stalls. Science 2003;302(5646):766–7.
[2] Guan Y, Zheng BJ, He YQ, Liu XL, Zhuang ZX, Cheung CL, et al. Isolation and characterization of viruses related to the SARS coronavirus from animals in southern China. Science 2003;302 (5643):276–8.
[3] Saif LJ. Animal coronaviruses: what can they teach us about the severe acute respiratory syndrome? Rev Sci Tech 2004;23(2): 643–60.
[4] Booth CM, Matukas LM, Tomlinson GA, Rachlis AR, Rose DB, Dwosh HA, et al. Clinical features and short-term outcomes of 144 patients with SARS in the greater Toronto area. JAMA 2003;289(21):2801–9.
[5] Chan JW, Ng CK, Chan YH, Mok TY, Lee S, Chu SYY, et al. Short term outcome and risk factors for adverse clinical outcomes in adults with severe acute respiratory syndrome (SARS). Thorax 2003;58(8):686–9.
[6] Donnelly CA, Ghani AC, Leung GM, Hedlev AJ, Fraser C, Riley S, et al. Epidemiological determinants of spread of causal agent of severe acute respiratory syndrome in Hong Kong. Lancet 2003;361(9371):1761–6.
[7] Lee N, Hui D, Wu A, Chan P, Cameron P, Joynt GM, et al. A major outbreak of severe acute respiratory syndrome in Hong Kong. N Engl J Med 2003;348(20): 1986–94.
[8] Peiris JS, Chu CM, Cheng VC, Chan KS, Hung IF, Poon LL, et al. Clinical progression and viral load in a community outbreak of coronavirus-associated SARS pneumonia: a prospective study. Lancet 2003;361(9371): 1767–72.
[9] Tsui PT, Kwok ML, Yuen H, Lai ST. Severe acute respiratory syndrome: clinical outcome and prognostic correlates. Emerg Infect Dis 2003;9(9):1064–9.
[10] Roberts A, Paddock C, Vogel L, Butler E, Zaki S, Subbarao K. Aged BALB/c mice as a model for increased severity of severe acute respiratory syndrome in elderly humans. J Virol 2005;79(9): 5833–8.
[11] Keller MA, Stiehm ER. Passive immunity in prevention and treatment of infectious diseases. Clin Microbiol Rev 2000;13(4): 602–14.
[12] Soo YO, Cheng Y, Wong R, Hui DS, Lee CK, Tsang KK, et al. Retrospective comparison of convalescent plasma with continuing high-dose methylprednisolone treatment in SARS patients. Clin Microbiol Infect 2004;10(7): 676–8.
[13] Subbarao K, McAuliffe J, Vogel L, Fahle G, Fischer S, Tatti K, et al. Prior infection and passive transfer of neutralizing antibody prevent replication of severe acute respiratory syndrome coronavirus in the respiratory tract of mice. J Virol 2004;78(7):3572–7.
[14] Lang J, Attanath P, Quiambao B, Singhasivanon V, Chanthavanich P, Montalban C, et al. Evaluation of the safety, immunogenicity, and pharmacokinetic profile of a new, highly purified, heat-treated equine rabies immunoglobulin, administered either alone or in association with a purified, Vero-cell rabies vaccine. Acta Trop 1998;70(3):317–33.
[15] Chiba T, Yokosuka O, Goto S, Fukai K, Imazeki F, Shishido H, et al. Successful clearance of hepatitis B virus after allogeneic stem cell transplantation: beneficial combination of adoptive immunity transfer and lamivudine. Eur J Haematol 2003;71(3):220–3.
[16] Dahmen U, Dirsch O, Li J, Fiedle M, Lu M, Rispeter K, et al. Adoptive transfer of immunity: a new strategy to interfere with severe hepatitis virus reinfection after woodchuck liver transplantation. Transplantation 2004;77(7): 965–72.
[17] Watt G, Kantipong P, Jongsakul K, de Souza M, Burnouf T. Passive transfer of scrub typhus plasma to patients with AIDS: a descriptive clinical study. QJM 2001;94(11):599–607.
[18] Ruprecht RM, Ferrantelli F, Kitabwalla M, Xu W, McClure HM. Antibody protection: passive immunization of neonates against oral AIDS virus challenge. Vaccine 2003;21 (24):3370–3.
[19] Wang X, Ni B, Du X, Zhao G, Gao W, Shi X, et al. Protection of mammalian cells from severe acute respiratory syndrome coronavirus infection by equine neutralizing antibody. Antivir Ther 2005;10(5):681–90.
[20] Giulietti A, Overbergh L, Valckx D, Decallonne B, Bouillon R, Mathieu C. An overview of real-time quantitative PCR: applications to quantify cytokine gene expression. Methods 2001;25(4): 386–401.
[21] Bhaskar G, Lodha R, Kabra SK. Severe acute respiratory syndrome (SARS). Indian J Pediatr 2003;70(5):401–5.
[22] Grinblat L, Shulman H, Glickman A, Matukas L, Paul N. Severe acute respiratory syndrome: radiographic review of 40 probable cases in Toronto, Canada. Radiology 2003;228(3):802–9.

[23] Muller NL, Ooi GC, Khong PL, Nicolaou S. Severe acute respiratory syndrome: radiographic and CT findings. AJR Am J Roentgenol 2003;181(1):3–8.
[24] Ooi GC, Daqing M. SARS: radiological features. Respirology 2003;8:S15–9 [Suppl].
[25] Paul NS, Roberts H, Butany J, Chung T, Gold W, Mehta S, et al. Radiologic pattern of disease in patients with severe acute respiratory syndrome: the Toronto experience. Radiographics 2004;24(2):553–63.
[26] Raoof S, Raoof S, Naidich DP. Imaging of unusual diffuse lung diseases. Curr Opin Pulm Med 2004;10(5):383–9.
[27] Peiris JS, Guan Y, Yuen KY. Severe acute respiratory syndrome. Nat Med 2004;10(12 Suppl):S88–97.
[28] Wang WK, Chen SY, Liu IJ, Kao CL, Chen HL, Chiang BL, et al. Temporal relationship of viral load, ribavirin, interleukin (IL)-6, IL-8, and clinical progression in patients with severe acute respiratory syndrome. Clin Infect Dis 2004;39(7):1071–5.
[29] Ho MS, Chen WJ, Chen HY, Lin SF, Wang MC, Di J, et al. Neutralizing antibody response and SARS severity. Emerg Infect Dis 2005;11(11):1730–7.
[30] Sui J, Li W, Murakami A, Matthews LJ, Wong SK, Moore MJ, et al. Potent neutralization of severe acute respiratory syndrome (SARS) coronavirus by a human mAb to S1 protein that blocks receptor association. Proc Natl Acad Sci U S A 2004;101(8):2536–41.
[31] Sui J, Li W, Roberts A, Matthews LJ, Murakami A, Vogel L, et al. Evaluation of human monoclonal antibody 80R for immunoprophylaxis of severe acute respiratory syndrome by an animal study, epitope mapping, and analysis of spike variants. J Virol 2005;79(10):5900–6.
[32] ter Meulen J, Bakker AB, van den Brink EN, Weverling GJ, Martina BE, Haagmans BL, et al. Human monoclonal antibody as prophylaxis for SARS coronavirus infection in ferrets. Lancet 2004;363(9427):2139–41.
[33] Traggiai E, Becker S, Subbarao K, Kolesnikova L, Uematsu Y, Gismondo MR, et al. An efficient method to make human monoclonal antibodies from memory B cells: potent neutralization of SARS coronavirus. Nat Med 2004;10(8):871–5.
[34] Duan J, Yan X, Guo X, Cao W, Han W, Qi C, et al. A human SARS-CoV neutralizing antibody against epitope on S2 protein. Biochem Biophys Res Commun 2005;333(1):186–93.